Chapter 7

Machine protection

D. Wollmann[1*], *R. Denz*[1], *B. Lindstrom*[1], *E, Ravaioli*[1], *F. Rodriguez Mateos*[1], *A. Siemko*[1], *J. Uythoven*[1], *A. Verweij*[1], *A. Will*[1] *and M. Zerlauth*[1]

[1]CERN, Accelerator & Technology Sector, Switzerland
[*]Corresponding author

7 Machine protection

Since the previous TDR version 0.1, the hardware development has made significant progress. The universal quench detection system, CLIQ and energy extraction system prototypes have been successfully produced and tested and first units have been successfully deployed and used in SM18. This progress is reflected in the Sections below and some of the previously retained options have therefore been removed. In addition, the development of the quench heater power supplies for the HL-LHC is well advanced, which is shown in the respective Section below. Chapter 6 was updated following the approval of layout changes to the triplet circuit and an additional Section on cold diodes was added, as they have been adopted within the HL-LHC baseline. Finally, two new sources for very fast failures have been identified and studied in the past years, which is presented in the Section on fast failures.

7.1 Overview

The combination of high intensity and high energy that characterizes the nominal beam in the LHC leads to a stored energy higher than in any previous accelerator. For nominal HL-LHC operation, the beam energy will increase by another factor of two compared to standard LHC parameters and, therefore, also significantly increase the damage potential due to accidental beam losses.

The damage limits of superconducting magnets due to instantaneous beam losses are currently under study, with two dedicated experiments performed in CERN's HiRadMat facility. First results clearly indicate that Nb_3Sn magnets are significantly more sensitive to damage by instantaneous beam losses than Nb-Ti magnets. For the latter, the allowed energy deposition to remain below the limit of any irreversible damage to the superconductor due to e.g. injection or dump failures is far beyond the specified 100 J/cm^3[1].

In addition, new beam loss failure scenarios are currently under study due to the experience from LHC Run 2, proposed optics changes, the installation of new accelerator components such as crab cavities or systems that might enter the HL-LHC baseline such as hollow electron beam lenses and long-range beam-beam compensators. Special care is required to define a trade-off between equipment protection and machine availability in view of the reduced operational margins (e.g. lower beam loss thresholds to assure a timely removal of the beam in view of increased beam intensity and tighter collimator settings, UFOs, etc.).

The new HL-LHC circuits will be protected by a newly developed universal quench detection electronics (UQDS), novel Coupling Loss Induced Quench (CLIQ) units, new energy extraction systems using in-vacuum electro-mechanical switches, re-designed quench heater power supplies and a new generation of radiation tolerant cold by-pass diodes.

7.2 New Fast Failures (Protection against uncontrolled beam losses)

Equipment failures or beam instabilities appearing on the timescale of tens of turns (with 1 LHC turn ~ 89 µs) allow for an active interlocking of beam operation by dedicated detection systems. These systems feature detection times of up to several hundred microseconds. The currently fastest detection systems are the LHC beam loss monitors (BLM, 80 µs) and the fast magnet current change monitors (FMCM, 20 µs). Following the detection of a failure, the beam interlock system (BIS) and the LHC beam dumping system (LBDS) will require less than 280 µs, or about three LHC turns, to complete the removal of the concerned beam from the LHC ring. Figure 7-1 depicts the time required, respectively allowed, from the occurrence of a critical failure or unacceptable beam loss until the completion of a beam dump. With this reaction time the accelerator can be protected against damage for failures, which do not cause critical beam loss levels in less than one millisecond or about 10 LHC turns.

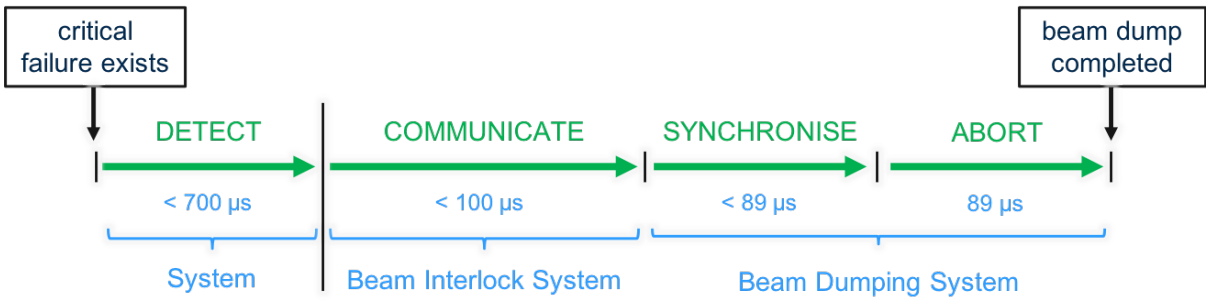

Figure 7-1: Sketch of the required machine protection system response time from existence of a failure to completion of the beam dump. These requirements allow the active interlocking of failures causing critical loss levels not faster than 10 LHC turns.

During LHC Run 2, small orbit oscillations of the circulating beam have been observed following quenches in the main dipole magnets. The magnetic field caused by the firing of the quench heaters, which protect the magnet from damage in case of a quench, has been confirmed in dedicated beam experiments and simulations to identify the origin of this orbit disturbance. Following an extremely fast increase in the first 270 µs these fields rise to the level expected from magnetostatic simulations after 1 ms [3][4]. Studies of the new HL-LHC magnets showed that the effect of their quench heaters on the beam will increase significantly as compared to today's LHC, due to the increased number of quench heaters and the drastically increased β-functions in the straight sections around IP1 and IP5. Therefore, the connection schemes of the quench heater circuits for the new HL magnets were optimised to reduce or, where possible, eliminate the skew dipole field created by the quench heater firing (see Table 7-1). Nevertheless, in case of the HL-LHC triplet magnets the total kick will still be unacceptable and a kick due to the spurious pre-firing of a single quench heater can reach critical levels. Therefore, in the new inner triplets of the HL-LHC it is required that the quench detection system initiates a beam dump before the firing of the quench heater circuits is triggered. A spurious firing of the quench heaters needs also to be interlocked triggering an immediate beam dump within ~ 1ms after the start of the discharge.

Table 7-1: Simulated kicks on the circulating beam due to firing of quench heaters in the LHC Run 2 and the HL-LHC in collision [4]. The values before the arrow in the HL-LHC column give the kick expected before the optimisation and the second value gives the kick after the optimisation.

Magnet (all QH)	LHC Run 2 kick [σ_{nom}]	HL-LHC kick [σ_{nom}]
Main dipole (worst case)	0.3	0.5
D1	1.4	2.0 → 1.4
D2	1.2	2.4 → < 0.3
11 T dipole	0.04	0.4 → 0.03
Triplet	2.5	33
Triplet (single QH – worst case)	0.6	1.2

As discussed in Section 7.3.1 the new HL-LHC triplet magnets are in addition to classical quench heaters protected by the novel CLIQ system. The connection scheme of this system is shown in Chapter 6. The spurious firing of one of the CLIQ systems in Q3 in collision will cause a very fast dI/dt in the different poles of the magnet. As this dI/dt is non-symmetric, it creates a fast-rising strong dipole kick, reaching an offset of about 3 σ_{nom} in the first turn and rising to more than 20 σ_{nom} within the first ten turns after the start of the firing process (see Figure 7-2 – left, Q3) [4]. This is an unacceptable failure which must be considered in the protection scheme. As mitigation, an alternative connection scheme has been identified, with one CLIQ unit protecting each half magnet of Q1 and Q3, as already done for Q2a and Q2b, in combination with a by-pass similar to the k-mod trim in Q1a. For this scheme, critical orbit offsets are reached only after 15 to 20 turns (see Figure 7-2 – right) [4]. Combined with a fast interlocking of a spurious firing of a CLIQ unit this scheme sufficiently reduces the criticality of this failure case to rely on the already foreseen active protection systems.

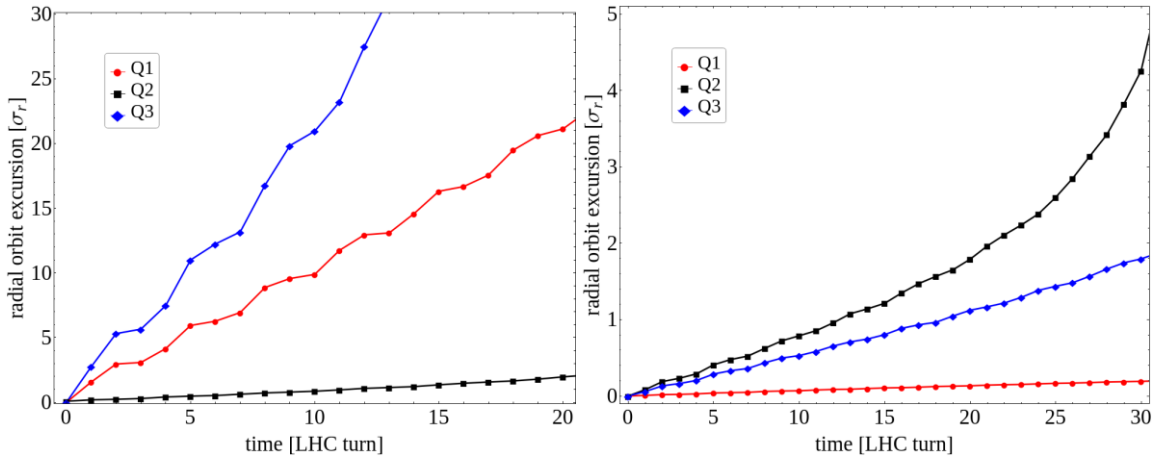

Figure 7-2: Left: The orbit excursion induced by a CLIQ discharge in the three triplet magnets Q1, Q2, and Q3. For each type, only the magnet with the largest kick is shown for the original connection scheme; Right: The orbit excursion induced by a CLIQ discharge using the new baseline in the three triplet magnets Q1, Q2 and Q3. For each type, only the magnet with the largest kick is shown in Ref. [4].

In a similar way as quench heaters and CLIQ, the use of crab cavities will introduce new failure scenarios that can affect the particle beams on timescales in the range of 10 turns [6]. Recent studies identified sudden phase changes in several crab cavities to be most critical, causing damage to the collimation system within less than five LHC turns [5]. Mitigation techniques of crab cavity failures have to include dependable detection of the crab cavity phase and voltage failures within less than 200 µs. In addition, correlated failures of multiple cavities (on one side of an IP) should be avoided through mechanical and cryogenic separation of the individual modules and appropriate design of the low-level RF.

Highly overpopulated transverse tails compared to the expected Gaussian beams were measured in the LHC (beam scrapings with collimators and van-der-Meer scans in the LHC experiments). Based on these observations, the energy stored in the tails beyond 4 σ are extrapolated to correspond to ~30 MJ for the HL-LHC parameters. These levels are significantly beyond the specification of the collimation system, with the present LHC design capable of absorbing up to 1 MJ for very fast accidental beam losses. The criticality of new fast failures can significantly be reduced by a partial depletion of the transverse beam halo, reducing the beam potentially being deflected into the collimation system to acceptable levels. Nevertheless, the impact of the halo depletion on the reaction time of the beam loss monitor system and, therefore, the protection in case of fast beam losses and possible mitigations via witness bunches needs to be carefully studied. In addition, if halo depletion is required for safe HL-LHC operation, it is mandatory to implement a reliable system to measure and interlock on the energy stored in the beam halo (see Chapter 5 on Hollow electron lenses).

7.2.1 Interlock Systems

The Beam Interlock System BIS is at the heart of CERN's accelerator machine protection systems. It is currently used in the LHC, SPS, LINAC4, and other parts of the injector chain at CERN. Its primary objective is to provide a fast and highly reliable link between users requesting a beam abort and the beam dumping system and injection elements. The hardware implementation of the system is based on custom-made electronics, as industrial solutions have not been found to be adequate for the specific requirements of the system, especially regarding the reaction time combined with the geographical distribution of the system. To fulfil the requirements of the HL-LHC, the system will be equipped with additional input channels to connect additional user interfaces and to provide more flexibility in the configuration of the various user inputs, while at the same time addressing shortcomings with the fibre optical links of the current LHC system. The number of required channels is subject to a future functional specification to be provided by the Machine Protection Panel (MPP). The new system will be equipped with advanced diagnostic features for all optical links allowing preventive maintenance, e.g. in the case of degraded performance due to the enhanced radiation load on the optical fibres in the underground areas.

The upgraded Machine Protection System will have to reach at least the same performance level in terms of reliability as the present system. For the Beam Interlock System this qualitatively corresponds to a likelihood of less than 10 % in 1000 years of operation of not transmitting a beam dump request. The safety critical part of the BIS hardware architecture will be based on well-proven principles and solutions but adapted to state-of-the-art electronic components and assemblies. From the availability point of view, the design goal of the new BIS hardware is not to cause more than one spurious beam abort per year, in line with the present operational system design and experience.

The new hardware, based on technologies like Small Form-factor Pluggable (SFP) and recent FPGA generations, will require a major revision of the high-level supervision and controls software and the adaptation to the accelerator controls environment as done at present.

7.3 Magnet circuit protection

The layout, circuit parameters as well as the protection method for the new HL-LHC circuits is described in Chapter 6 of this report. In the following Section, the quench protection of the new triplet circuit and the chosen technical solutions for quench detection systems, quench heater powering, coupling loss induced quench systems, energy extraction systems, cold by-pass diodes and the powering interlock controllers will be discussed.

7.3.1 Quench protection of the new inner triplet circuits

The new triplet quadruple magnets for the HL-LHC are wound using Nb_3Sn Rutherford cables. It was decided to keep the maximum hotspot temperatures below 350 K during quenches in nominal conditions. In rare failure scenarios the hotspot can reach up to 380 K. The quench protection scheme of these triplet circuits is aiming for the lowest possible hot-spot temperatures and thermal gradients, and sufficiently low voltages to ground and inter-turn and inter-layer voltages (see Chapter 6). To achieve these goals, each magnet will be equipped with 16 quench heater strips (8 in the low-field and 8 in the high-field regions), which will be powered in 8 heater circuits. In addition, the circuit will be protected with CLIQ units, which will reduce peak temperatures in the triplet magnets and add diverse redundancy of protection wrt to the quench heater circuits (see 7.3.4). Each single magnet (Q1a, Q1b, Q2a, Q2b, Q3a, Q3b) will be equipped with one CLIQ unit. In total, this corresponds to 48 quench heater circuits and 6 CLIQ units per triplet. Note, that this describes the baseline protection scheme of the new triplet circuits. The performance of the protection systems has so far been validated in short model coils, and on the first MQXFA magnet prototype by US-AUP (4 m long) but remains to be validated for longer prototypes and in the IT string. Cold parallel diodes (see 7.3.6) minimize the voltages in the circuit during a quench in case of non-zero currents in the trim circuits and differing discharge rates in the individual triplet quadrupoles due to tolerances and possible failures.

Detailed quench protection studies, including sensitivity studies of the superconductor parameters and failure cases, have been performed for the triplet circuit, i.e. MQXFA and MQXFB, and are summarized in Refs. [7] [9]. Table 7-2 summarizes the simulated worst-case hot spot temperatures and peak voltages to ground during a quench with nominal protection by quench heaters and CLIQ for the two magnet types. The given parameter range indicates the spread of the simulation results depending on the quench location and the variation of cable parameters within their specifications. It can be clearly seen that the hot spot temperature stays well below the specified 350 K.

Table 7-2: Simulated worst-case hot spot temperature (T_{hot}), peak voltage ($U_{g,peak}$) to ground and peak turn to turn voltage ($U_{t,peak}$) obtained after a quench at nominal and ultimate current for varying copper to superconductor rations, RRR and strand diameter. The range also includes the effect of different quench locations [7]. The ranges presented include MQXFA and MQXFB.

Current	**T_{hot} (K)**	**$U_{g,peak}$ (V)**	**$U_{t,peak}$ (V)**
I_nominal	215 – 248	521 – 658	49 – 90
I_ultimate	237 – 273	664 – 924	61 – 109

Figure 7-3 shows the typical currents in the triplet circuit (main circuit branch, trim Q1, trim Q3 and k-modulation trim) and the cold diodes during a quench at nominal current. The development of the hot spot temperature and the currents in poles P2-P4 and P1-P3 during a quench of magnet Q2a is depicted in the left plot of Figure 7-4. The right plot of Figure 7-4 shows the envelop of the voltages to ground in the coil (min and max) in case of a quench at nominal current.

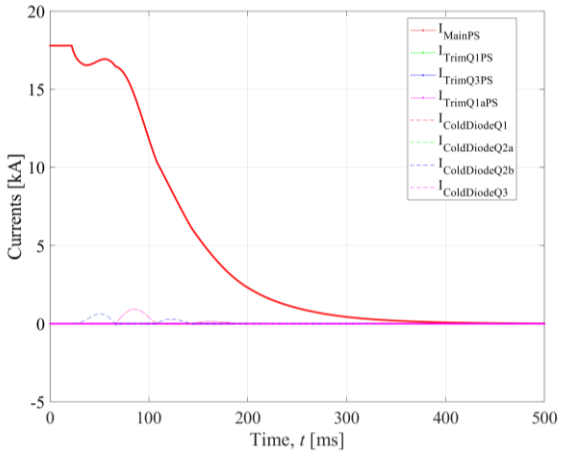

Figure 7-3: Typical current in the different branches of the triplet circuit and the cold diodes during a quench at nominal current. The simulation results were derived from STEAM-COSIM, coupling a STEAM-LEDET [30] magnet model to a PSPICE© electrical circuit model.

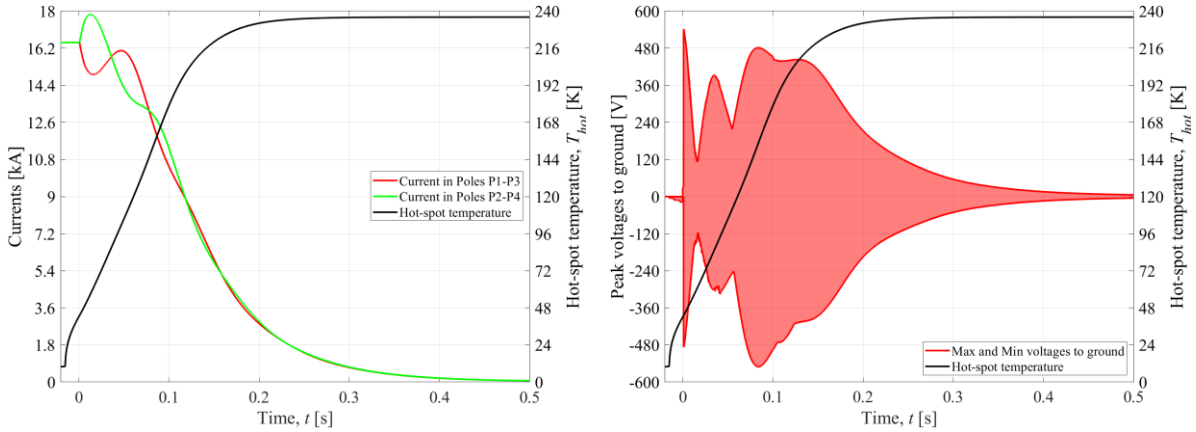

Figure 7-4 Left: currents in poles P1-P3 and P2-P4 during a quench of magnet Q2a (Q2 being of the longest type) and development of the hot spot temperature. Right: Envelop of the voltages to ground in the coil (min and max) and development of hot spot temperature in case of a Q2a quench at nominal current. The simulation results were derived from STEAM-LEDET [30].

7.3.2 Quench detection system

The HL-LHC project will incorporate for its magnet powering system a new generation of superconducting elements such as high field superconducting magnets based on Nb_3Sn conductors and high temperature superconducting links based on MgB_2. In addition, the HL-LHC will also feature new generations of Nb-Ti based magnets. The proper protection and diagnostics of those elements requires the development of a new generation of integrated quench detection and data acquisition systems (QDS). For the HL-LHC QDS, a unified approach, the Universal Quench Detection System (UQDS) described in Ref. [12] will be used.

7.3.2.1 UQDS general architecture

As a flexible and generic system, the UQDS architecture is not bound to a specific quench detection algorithm and can be configured according to the requirements of the protected superconducting element. In case of the HL-LHC, the UQDS can be adapted to the needs of various magnet technologies and provide as well efficient protection for the novel MgB_2 high current cable links. One of the key elements of the UQDS architecture are the analogue front-end channels, which are equipped with a high-resolution analogue to digital converter (ADC) of the successive approximation type. Insulated DC-DC converters and digital isolators for the serial data interfaces provide galvanic isolation of the analogue channels. In the current implementation, up to 16 of such channels connect to a field programmable gate array (FPGA), which processes the acquired data and executes the quench detection algorithms. The isolated nature of the analogue front-end channels allows a flexible usage of the magnet instrumentation, as there is no limitation imposed in the comparison of voltages by differences in common-mode potential. To enhance reliability, UQDS units (see Figure 7-5) are always deployed as a set of two independent units reading signals from two redundant sets of instrumentation voltage taps. Each unit is powered by two independent and monitored power supply units, which are supplied by different uninterruptable power supply (UPS) rails. The UQDS units are equipped with dedicated hardware interlocks for the activation of the protection elements of the magnet circuit such as quench heater discharge power supplies (DQHDS), Coupling Loss Induced Quench units [22] and energy extraction systems. The built-in field-bus interface, either of the WORLDFIP™ or the POWERLINK™ standard, provides the data link to the front-end computers of the accelerator control system.

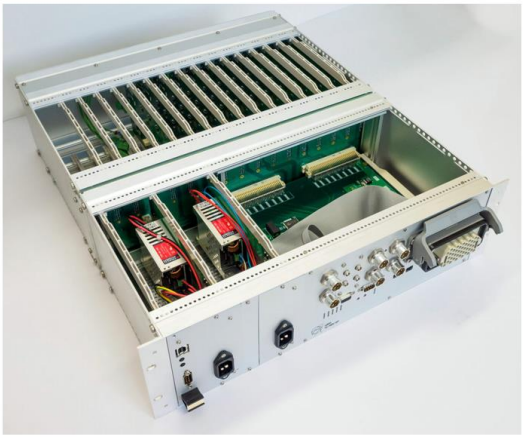

Figure 7-5: UQDS v2.1 crate serving as the baseline prototype for the 11T quench detection system. The crate is not equipped with top covers to illustrate its construction.

7.3.2.2 Quench detection for 11 T dipole magnets

The Nb_3Sn based 11T dipole magnets of type MBH will be installed in series to the main bending dipoles of LHC in sectors 6-7 and 7-8. Located in the dispersion suppressor region of both sides of IP7, the shorter but stronger 11T magnet will provide space to insert additional collimators (see also Chapters 5 and 11). The quench detection algorithm [23] uses a complex scheme, where an insulated channel measures the voltage over each pole and adjacent bus-bars. The bus-bars between the two magnet halves are protected via two additional channels. Comparisons between poles of the physically separated submodules MBHA and MBHB serve as an efficient method to detect aperture symmetric quenches that might arise due to beam losses in this region. To increase the reliability of quench detection, the scheme is implemented in a fully redundant way using the redundant voltage taps on the magnet level (see Figure 7-6). To cover all pieces of superconductor in a redundant scheme, the pole voltages include the adjacent pieces of bus-bars in an overlapping way.

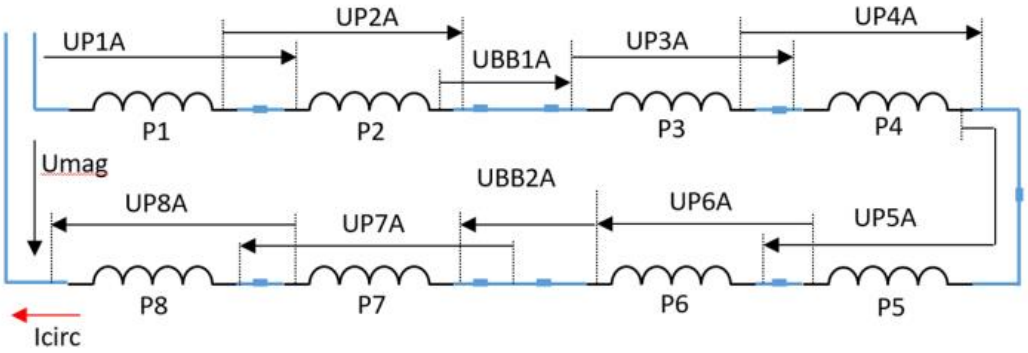

Figure 7-6: Simplified schematic of the 11T magnet circuit. The arrows indicate the voltages measured for one redundancy level. To cover all superconducting elements, the voltage measurements are interleaved.

Nb_3Sn based magnets experience so-called flux jumps [24], which result in voltage spikes on the magnet poles which are also directly seen by the quench detection electronics. The quench detection algorithm needs therefore to be adapted in order to reduce its sensitivity to these transient signals to reduce the likelihood of false positives. Since flux jumps are more dominant at lower currents where protection requirements are less stringent, a suitable solution is the application of current dependent detection settings. For this purpose, the UQDS unit is equipped with an adequate system for reading the circuit current.

In case of the 11T dipole, the 16 quench heater power supplies (DQHDS) feeding the quench heaters [25] are located close to the magnet and are triggered by the UQDS quench controllers. To activate the energy extraction systems and to switch off power converters in case of a quench the QDS system simultaneously opens the quench interlock loop of the main dipole circuit. From an LHC machine protection view, it is important to dump the beams prior to the quench heater activation. To comply with this requirement the quench loop controllers in sectors 6-7 and 7-8 will be upgraded for faster reaction and transmission times towards the subsequent powering and beam interlock systems.

7.3.2.3 11 T trim circuit protection

The resistive current leads and the superconducting bus-bars of the 11 T trim circuits require an active detection system to prevent overheating. The quench detection system measures the voltage drop across the resistive leads including the superconducting bus-bar and verifies the current sharing between the two individual leads of each circuit polarity.

7.3.2.4 Quench protection for new inner triplets in IR1 and IR5

The quench detection algorithms for the inner triplet circuits follow the same principles as for the protection of the 11 T dipoles. Due to the complexity of the triplet circuit, the number of required channels for quench detection is significantly higher (see Table 7-3). All quench detection systems for the inner triplet, the D1 magnet and the corrector package will be installed in the new, shielded underground areas UR1 and UR5 and are therefore not required to be radiation tolerant.

Table 7-3: Signals for Inner Triplet Protection (per circuit). Some channels use also share pole voltage taps. The possible dedicated detection for return bus-bar Q1-Q3 is not yet included.

Signal type	**Vtaps**	**UQDS channels**
Pole voltage	96	48
Bus-bar voltage	20	18[1]
Current	N/A	6
Earth voltage	N/A	6
Corrector voltage	24	16
Corrector bus-bar voltage	16	16
Corrector current	N/A	8
Corrector current derivative sensors	N/A	8
Sum	**156**	**126 (10 units)**

7.3.2.5 Inner triplet quench heater circuit and CLIQ supervision and triggering

The supervision and triggering of the quench heater power supplies (DQHDS) and CLIQ units is managed by a dedicated supervision and trigger controller (DQHSU). The DQHSU records data from quench heater and CLIQ discharges with sampling rates up to 192 kS/s and ensures the timely activation of the DQHDS and CLIQ units. For safe LHC operation, it is mandatory to dump the beams prior to the quench heater activation. A spurious trigger of a CLIQ unit and a DQHDS requires an immediate beam abort combined with a re-trigger of all not yet activated CLIQ and DQHDS units (see Table 7-4).

Table 7-4: Timing of beam abort sequence in case of spurious quench heater or CLIQ activation [10].

Step	**Duration**
Detection DQHDS (di/dt ≈ 4 MA/s)	100 µs
Detection CLIQ (di/dt ≈ 200 kA/s)	< 500 µs
Communication DQHSU → PIC → BIS [x]	12 µs
Beam abort sequence	270 µs
Total	**< 1 ms**

7.3.2.6 Quench detection systems for MgB_2 based high temperature superconducting links

For the protection of the MgB_2 multi-cable assemblies, which incorporate cables with current ratings from 2 kA to 18 kA, dedicated quench detection units will be deployed. The same UQDS electronic is used, while detection algorithms and thresholds will be adapted according to the needs of this new material technology. In case triggered, the UQDS systems trigger a power abort and the active protection systems of the respective circuit such as CLIQ units, DQHDS or energy extraction systems. For each pair of cables, the UQDS triggers on the differential voltage signal as well as on the absolute voltage signal as symmetric quenches in a pair of cables cannot be excluded.

7.3.2.7 Quench detection systems for D1, D2 and D2 orbit correctors

The new Nb-Ti D1 and D2 magnets will also be protected with the UQDS quench detection systems. In addition, separate bus-bar and link protection, enhanced quench heater supervision and current derivative sensors for symmetric quench detection will be installed. Furthermore, the new CCT type D2 correctors require as well, the deployment of a UQDS unit for their protection. For safe LHC operation, it is mandatory to dump the beams prior to the activation of quench heaters in the D1 and the D2.

7.3.2.8 HL-LHC impact on existing quench detection electronics

The enhanced luminosity of the HL-LHC will increase the radiation levels in the dispersion suppressor regions around IP1 and IP5 to levels requiring an upgrade of the quench detection electronics currently installed in those areas. The latest simulations indicate a total integrated dose of up to 100 Gy/year in some locations [8]. For these integrated dose levels, it is still possible to develop enhanced, more radiation tolerant versions of the currently installed QDS electronics using qualified Commercial of the Shelf (COTS) components.

With the high intensity beams of the HL-LHC, the risk of beam induced symmetric quenches in the insertion region magnets is significantly increased. The deployment of the novel current derivative sensors, which allow for an elegant method of quench detection, is considered as an adequate solution to overcome the limitations of the presently installed systems.

Another possible application of current derivative sensors are the quench detection systems for the closed orbit correctors of the inner triplets in IP2 and IP8. In this case, the current derivative sensors will allow better inductive compensation and in consequence higher ramp rates and acceleration for these circuits.

7.3.3 Quench Heater Power Supplies

The Quench Heater Discharge Supplies (DQHDS), widely known as Quench Heater Power Supplies, are the units responsible for energizing the quench heaters strips installed on the magnet coils in order to dissipate the energy stored in the magnet into its full volume, hence limiting the hot-spot temperature at the location of the original quench and preventing damage to the coil.

Every DQHDS consists of a capacitor bank with 6 aluminium electrolytic capacitors (4.7 mF/ 500 V) arranged in two sets of 3 capacitors each, which are connected in series, resulting in a total capacitance of 7.05 mF / 1000 V. The nominal operating voltage of the capacitors will be 450 V and therefore an overall voltage for the capacitor bank of 900 V is expected to deliver ~3.5 kJ to a single quench heater strip when the unit is triggered by the QDS. Figure 7-7 shows a simplified scheme of a DQHDS.

Presently, there are over 6000 DQHDS installed in the LHC and an additional ~320 DQHDS with improved capabilities and higher reliability will be needed for the HL-LHC in order to protect the 11T dipoles, the Inner Triplet quadrupoles and the new separation and re-combination dipoles D1 and D2.

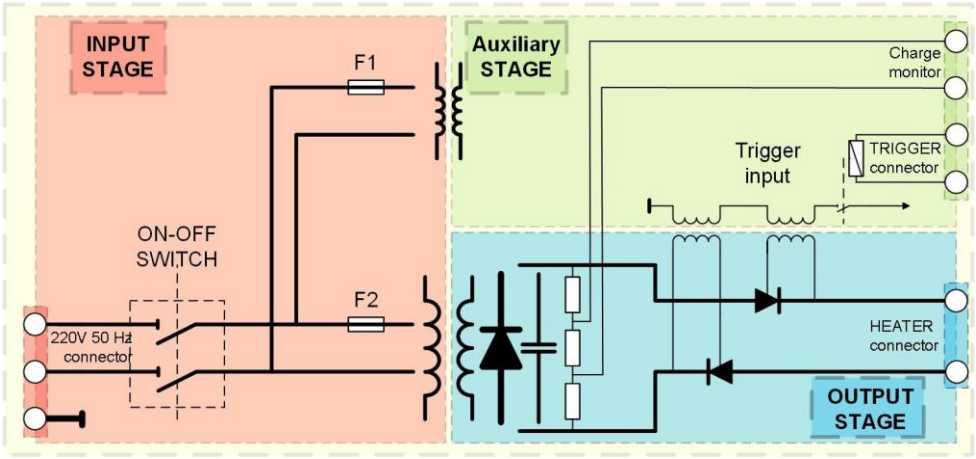

Figure 7-7: Simplified electrical scheme of a DQHDS unit

The 11T cryo-assemblies, as well as the protection racks, will be installed during LS2. Figure 7-8 shows the prototype of the DQHDS units prepared for the 11 T magnet. In the meantime, the series units have been produced and qualified. The DQHDS dedicated to the protection of the Inner Triplet and Matching section will be installed during LS3 and a first prototype is currently under development.

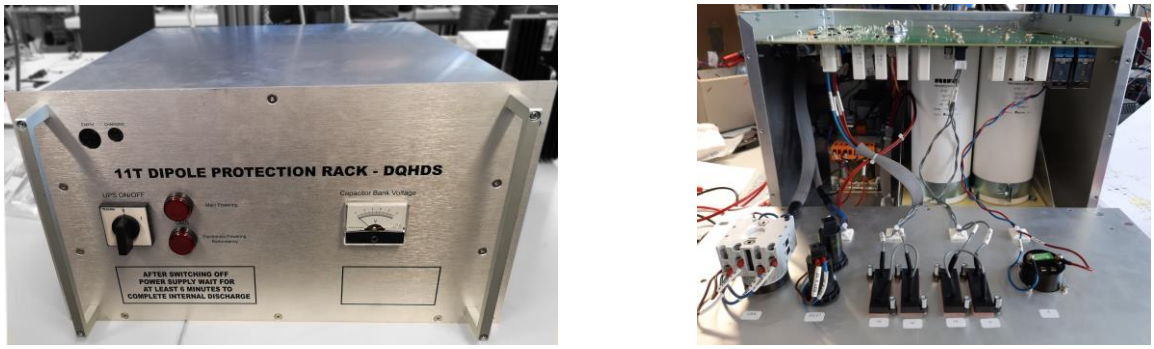

Figure 7-8: Prototype of a DQHDS for the 11T Magnet. In the right picture shows the DQHDS unit with open front face. Two of the total six capacitors can be clearly seen (white cylinders).

7.3.4 Coupling-Loss Induced Quench (CLIQ)

Coupling-Loss Induced Quench (CLIQ) is an innovative method for the protection of superconducting magnets after a quench [13][14][15]. Its fast and effective heating mechanism, utilizing coupling loss between the conductors of the coil, and its robust electrical design makes it a very attractive solution for high-field magnets. The CLIQ technology has been already successfully applied to magnets of different size, coil geometry, and type of superconductor.

The CLIQ system is schematized in Figure 7-9. It is composed of a capacitor bank C, a floating voltage supply S, two additional resistive current leads CL1 and CL2 connecting the system to the magnet, and a Bidirectional Controlled Thyristor (BCT) package, indicated as TH in the figure. The positioning of the connection of the current leads strongly affects the effectiveness of the CLIQ system. These leads carry typically 10% of the nominal magnet current for about 100-200 ms and can therefore have a small cross-section. The capacitor bank is charged by the power supply S with a voltage U_C. Upon quench detection, the bi-directional thyristors are activated resulting in a current I_C being discharged through CL2 leading initially to an over-current in P2-P4 and an under-current in P1-P3 as compared to the nominal current in the magnet (see Figure 7-10). The BCT package allows for several oscillations of these currents.

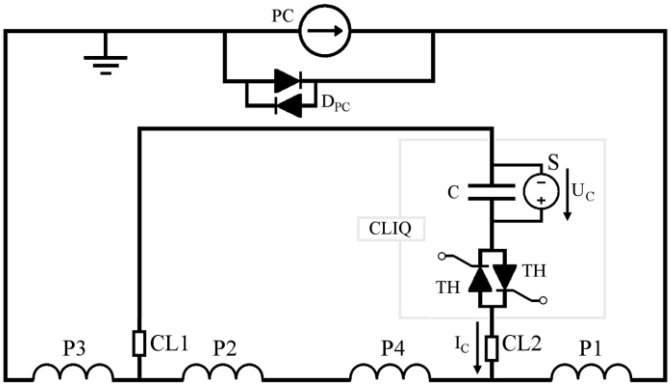

Figure 7-9: Schematic of a CLIQ unit connected to a magnet for its protection [13].

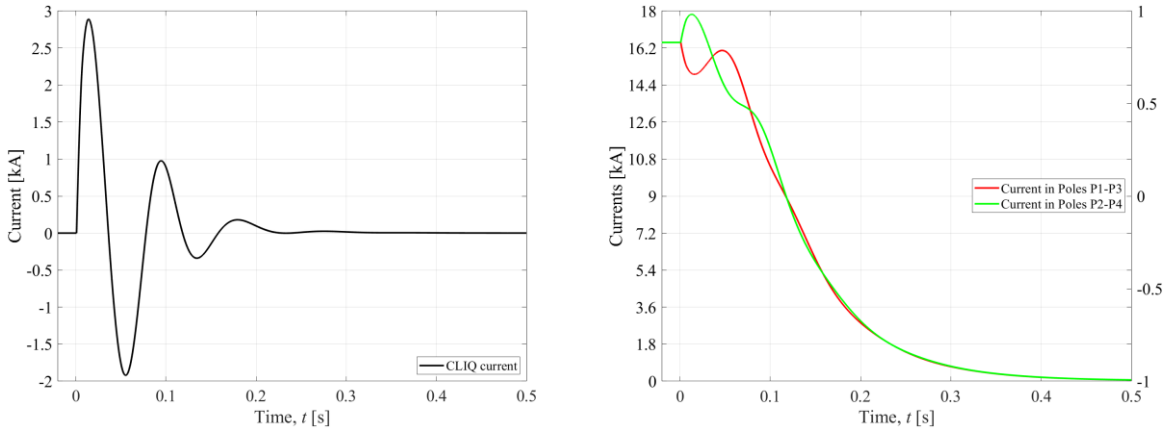

Figure 7-10: Oscillation of the CLIQ current I_c (left) and resulting overall current in the poles of the magnet (right) following the activation of the CLIQ thyristors as simulated with STEAM-LEDET [30].

CLIQ in combination with the DQHDS and quench detection system assures that the peak temperatures and voltages to ground in the MQXF coils are maintained within safe limits. A detailed analysis of the magnet quench protection of the inner triplet circuits can be found in Ref. [15]. The CLIQ units connected to the magnets must comply with the same standards as quench heaters. As the units are directly connected to the magnet potential, every effort must be made for reducing the probabilities of a short circuit across a unit or internally within a unit.

So far 11 CLIQ units of industrial-grade have been manufactured and successfully qualified [17] while the machine version, that will include an improved monitoring and interlock system, enhanced electronics and a higher reliability configuration, is being designed at this moment. Figure 7-11 shows units of the second-generation prototypes, manufactured for the tests of the inner triplet magnets in SM18.

A validation programme using prototype CLIQ units, on the HL-LHC model and prototype magnets, has been successfully carried out within the different magnet test programmes [18][19].

Figure 7-11: CLIQ prototype units of the second generation in the MPE test lab

7.3.5 Energy extraction system

Energy extraction (EE) systems are an important part of the safety-critical quench protection equipment, which are widely used in the existing LHC machine for fast discharge of the energy stored in its superconducting magnet circuits in case of quench. Their design, based on specific and conservative sets of requirements, ensures a reliable dissipation (extraction) of the stored energy that may otherwise overheat and even damage the quenching superconducting parts of the circuit. Currently, 234 energy extraction systems of two distinct types are installed in the LHC machine:

- 202 systems that protect the 600 A-class corrector magnet circuits.
- 32 systems for the main 13 kA dipole and quadrupole circuits.

The existing installations use high-speed electromechanical DC circuit breakers to commutate upon request the circuit current into one or several dedicated energy absorbers (dump resistors). The resistors are permanently connected in parallel to the breakers, passively waiting the opening of the switches to start dissipating the magnet's energy. This basic protection principle is going to be kept the same in the forthcoming HL-LHC.

The present 13kA EE systems will continue their operation after an extensive consolidation program performed on their power and control parts. The dump resistors will be kept the same as well, with resistance values of 2×75 mOhms for dipole systems and 6.8/7.7 mOhms for quadrupole systems. This limits the maximum current decay rate to -125 A/s in the dipole circuits and defines the extraction time constant to 104 sec for dipoles and 37 sec for quadrupoles circuits.

The 600A EE systems will have to be entirely consolidated for the HL-LHC era, introduce at the same time another DC switching technology. Fast vacuum switches will replace the conventional electromechanical devices, providing almost 10 times faster opening times. The new switches will be assembled with two in series, being fully independent from one another. They are practically maintenance-free, requiring only 1 to 2 interventions for the whole of their service life which is estimated to more than 20 000 cycles. The new energy dissipation resistors are composed of two units. They are identical and connected in parallel to the switches. The resistors are industrially made, compact, with low internal inductance devices, each with a resistance of 1.4 Ohms, and a rated energy deposition of 150 kJ. The replacement of the present systems is currently planned in a staged manner between LS3 and LS4.

In parallel with the consolidation and renewal of the existing EE systems, the HL-LHC requires the installation of additional 44 completely new systems for the protection of the MCBXFA/B, MQSXF and MCBRD corrector magnet circuits. The circuits containing MQSXF and MCBRD will be equipped with the 600A vacuum switch-based EE systems as their ultimate current is compatible with this rating. A suitable

resistor in accordance with the circuit specification will be selected and this will be the only different element with respect to the other EE systems using vacuum switches.

Regarding the MCBXFA/B circuits, a third-class EE facility rated for 2kA will be put in operation, as the nominal current flowing in these circuits is 1.6 kA. These EE systems also will be based on vacuum switches with slightly different operational parameters but the same topology as the 600A ones. Four resistors of 0.3 Ohms and 250kJ of nominal energy dissipation capacity will be connected in two parallel branches to provide safe dissipation of the energy when required. Figure 7-12 shows the first prototype of the 2 kA EE system for the HL-LHC.

Figure 7-12: Prototype of 2 kA EE system based on vacuum breakers. Left: rack of first prototype; Right: Zoom on vacuum switch and auxiliary components

The new energy extraction equipment for the HL-LHC will use a new generation of DC switches, which incorporates the latest technology for high-current transmission. The equipment will benefit from improved diagnostics and requires significantly less maintenance.

7.3.6 Cold diodes for the IT circuit

The complexity of the Inner Triplet circuits of the HL-LHC calls for the installation of cold diodes in parallel to magnets Q1, Q2a, Q2b and Q3 (see Fig. 6-4 of the circuit in Chapter 6). These diodes will be located in a dedicated extension cryostat between D1 and the DFX, immersed in superfluid helium, and hence not be located very far from the beam axis. As opposed to the previous option of warm diodes, which would have been located in the new UR cavern, the cold diodes will avoid large over-currents through the superconducting link in case of non-uniform quenches across the different magnets. Furthermore, the cold diodes avoid large voltages in between magnets, and give more robustness to the whole circuit system, allowing to better cope with the differences between magnets and cable parameters (RRR, Cu/SC ratio, strand diameter) as well as increasing the available times for the detection and protection devices (quench detectors, CLIQ, quench heater power supplies).

However, the cold diodes will be exposed to high radiation doses and fluence of neutrons and high energy hadrons, leading to a potential degradation of their characteristics over time. The integrated radiation dose and fluence at the location of the cold diodes is estimated to reach up to 12 kGy and 5×10^{13} n/cm^2 1 MeV equivalent over the HL-LHC lifetime [20].

The radiation tolerance of different types of bypass diodes has been tested at low temperatures at CERN's CHARM irradiation facility during the operational year 2018. The main electrical properties of the diodes (turn-on voltage, forward voltage, reverse blocking voltage and capacitance) have been measured on a

weekly basis, at 4.2 K and 77 K, respectively, as a function of the accumulated dose/fluence. The diodes were submitted to an integrated dose close to 12 kGy and a 1 MeV equivalent neutron fluence of 2.2×10^{14} n/cm^2. After the end of the irradiation campaign, the annealing behaviour of the diodes was tested by increasing the temperature to 300 K. The diodes' electrical properties gave satisfactory results and have been added to the HL-LHC baseline following their successful qualification [21].

7.3.7 Powering interlock system (PIC)

The powering interlock system PIC guarantees the presence of the correct powering conditions for the electrical circuits with superconducting magnets in the LHC. At the same time, it guarantees the protection of the magnet equipment by interfacing the quench protection systems, the beam interlock system, the power converters, the cryogenic system, and technical services such as uninterruptable power supplies (UPS), emergency stop buttons (AUG), and controls. The PIC is a distributed system consisting for the current LHC of 36 individual powering interlock controllers, which manage the powering of each of the 28 powering subsectors [8]. Note, that the arcs require two PICs per powering subsector.

The PIC is a hybrid system consisting of a central, standard PLC connected to deported Input – Output units via a specific electronic board, including an industrial PROFIBUS-DP interface and a CPLD, close to the equipment they are connected to. The PLCs are installed in the UA and UL areas, where acceptable levels of radiation are expected, while the deported Input – Output units in IP1, IP5 and IP7 are installed in the RRs and are subjected to radiation. The PLCs are not radiation tolerant, while the deported I/O units have been successfully tested to withstand low radiation levels, as foreseen in the original design 15 years ago.

At the design luminosity for the HL-LHC (5×10^{34} cm^{-2} s^{-1}), and even more for ultimate, the thermal neutron and high-energy hadron fluencies in the areas close to the tunnel, like the RRs, will increase considerably with respect to the values for which the existing PIC has been designed and tested. In IP1 and IP5, a relocation of the PLCs from the UL/USC areas to the new UR galleries is under study. For IP1, IP5 and IP7 no repositioning of the deported I/Os units from the RRs is foreseen. The estimate of the increased radiation levels for the HL-LHC is above the acceptable level of the deported PIC units. For this reason, a new version of the PIC deported units is foreseen, based on radiation tolerant FPGAs, up to the levels predicted for the HL-LHC with ultimate luminosity operation. The upgrade will also cover the refurbishment of the electronics, which has become obsolete and is expected to reach its end of life in the coming years. The replacement of the central PLC is also under study.

The new PIC system will have exactly the same functional specification as the present PIC and the interfaces to the different systems are not expected to change considerably. The protection of the new 11 T dipole magnets, which includes a new dipole trim circuit, can be covered by the present functionality. This trim circuit will be treated in the same way as other corrector circuits in the LHC.

Table 7-4 summarizes the interlock requirements for the RB circuits 6-7 and 7-8 and the related 11 T trim circuit [27]. The Trim circuit will be considered as essential from the PIC side, which means un-maskable at the level of the beam interlock controller (BIC).

Table 7-4: Interlock requirements for the RB circuits in sectors 6-7 and 7-8 including the 11 T trim circuit [27].

Interlock case	**PIC Action on RB Circuit**	**PIC Action on Trim Circuit**	**Beam Dump**
Quench in RB circuit	Fast Power Abort	Fast Power Abort	Yes
RB Discharge Request	Fast Power Aboort	Fast Power Abort	Yes
Powering Failure in RB Circuit	Slow power Abort	No action	Yes
Current Lead of Trim circuit	No action (Fast Power Abort triggered by QDS)	Fast Power Abort	Yes
Powering Failure in Trim Circuit	No action	Slow Power Abort	Yes
Switch opening request by RB PC	Fast Power Abort	Fast Power Abort	Yes
Cryo-failure	Slow Power Abort	Slow Power Abort	Yes

7.4 References

[1] V. Raginel, M. Bonura, D. Kleiven, K. Kulesz, M. Mentink, C. Senatore, R. Schmidt, A. Siemko, A. Verweij, A. Will, and D. Wollmann, "First Experimental Results on Damage Limits of Superconducting Accelerator Magnet Components Due to Instantaneous Beam Impact", IEEE Trans. Appl. SC, Vol 28(4), June 2018, DOI: 10.1109/TASC.2018.2817346.

[2] V. Raginel, "Study of the Damage Mechanisms and Limits of Superconducting Magnet Components due to Beam Impact", CERN-THESIS-2018-090.

[3] M. Valette, L. Bortot, A. Fernandez Navarro, B. Lindstrom, M. Mentink, E. Ravaioli, R. Schmidt, E. Stubberud, A. Verweij, D. Wollmann, "Impact of superconducting magnet protection equipment on the circulating beam in HL-LHC", IPAC 2018, DOI: 10.18429/JACoW-IPAC2018-THPAF062.

[4] B. Lindstrom, P. Belanger, L. Bortot, R. Denz, M. Mentink, E. Ravaioli, F. Rodriguez Mateos, R. Schmidt, J. Uythoven, M. Valette, A. Verweij, C. Wiesner, D. Wollmann, M. Zerlauth, "Fast failures in the LHC and the future high luminosity LHC", Phys. Rev. Accel. Beams 23 (2020) 081001, DOI: 10.1103/PhysRevAccelBeams.23.081001.

[5] A. Santamaria Garcia, "Experiment and Machine Protection from Fast Losses caused by Crab Cavities in the High Luminosity LHC", CERN-THESIS-2018-142.

[6] T. Baer *et al*., "Very fast crab cavity failures and their mitigation", Proc. IPAC'12, May 2012, pp. 121–123, MOPPC003, CERN-ATS-2012-106.

[7] E. Ravaioli, "Quench protection studies for the high luminosity inner triplet circuit", EDMS: 1760496.

[8] R. Schmidt B.Puccio, M.Zerlauth, "The hardware interfaces between the powering interlock system, power converters and quench protection system", EDMS: 68927.

[9] E. Ravaioli, G. Ambrosio, B. Auchmann, P. Ferracin, M. Maciejewski, F. Rodriguez-Mateos, GL. Sabbi, E. Todesco, A. Verweij: "Quench Protection System Optimization for the High Luminosity LHC Nb_3Sn Quadrupoles", IEEE Trans. on Appl. SC, 2017, DOI: 10.1109/TASC.2016.2634003.

[10] A. Antoine, "Study of the delay time required by the PIC to do a beam dump request", EDMS: 2187812.

[11] L. Rossi, (ed.) and O. Brüning (ed.), "The High Luminosity Large Hadron Collider : the new machine for illuminating the mysteries of Universe", World Scientific, Hackensack, 2015, DOI: 10.1142/9581.

[12] R. Denz, E. de Matteis, A. Siemko, J. Steckert, "Next Generation of Quench Detection Systems for High Luminosity Upgrade of the LHC", ASC'2016, 2016, DOI: 10.1109/TASC.2016.2628031.

[13] E. Ravaioli, CLIQ. "A new quench protection technology for superconducting magnets", PhD thesis University of Twente, 2015, CERN-THESIS-2015-091.

[14] V.I. Datskov, G.Kirby, and E. Ravaioli, "AC-Current Induced Quench Protection System", EP13174323.9, Application Granted 2020-03-25.

[15] E. Ravaioli *et al.,* "Advanced Quench Protection for the Nb_3Sn Quadrupoles for the High Luminosity LHC", IEEE Trans. Appl. Supercond. 26, 2016, DOI: 10.1109/TASC.2016.2524464.

[16] Conceptual Design Review of the Magnet Circuits for HL-LHC, 21.-23.03.2016, CERN, Switzerland. INDICO: 477759.

[17] F. Rodriguez Mateos, S. Balampekou, D. Carrillo, K. Dahlerup-Petersen, M. Favre, J. Mourao and B. Panev, "Design and Manufacturing of the First Industrial-Grade CLIQ Units for the Protection of Superconducting Magnets for the High-Luminosity LHC Project at CERN," in IEEE Transactions on Applied Superconductivity, vol. 28, no. 3, DOI: 10.1109/TASC.2018.2794473.

[18] E. Ravaioli, V. I. Datskov, G. Dib, A.M. Fernandez Navarro, G. Kirby, M. Maciejewski, H. H. J. ten Kate, A. P. Verweij and G. Willering, "First Implementation of the CLIQ Quench Protection System on a 14-m-Long Full-Scale LHC Dipole Magnet" IEEE Trans. On applied Superconductivity, vol. 26, No4, 2016, DOI: 10.1109/TASC.2015.2510400.

[19] E. Ravaioli, G. Ambrosio, H. Bajas, G. Chlachidze, P. Ferracin, S. Izquierdo Bermudez, P. Joshi, J. Muratore, F. Rodriguez-Mateos, GL. Sabbi, S. Stoynev, E. Todesco, and A. Verweij, "Quench

protection performance measurements in the first MQXF magnet models", IEEE Trans. Appl. Supercond., DOI: 10.1109/TASC.2018.2793900.

[20] G. Lerner, R. G. Alia, M. S. Gilarte, A. Tsinganis, and F. Cerutti, "Update on HL-LHC radiation levels on equipment in the IP1-IP5 LSS", presentation at the 9th HL-LHC Collaboration Meeting, Fermilab, USA, 15 October 2019, INDICO: 806637.

[21] A. Will, G. D'Angelo, R. Denz, D. Hagedorn, A. Monteuuis, E. Ravaioli, F. Rodriguez-Mateos, A. Siemko, K. Stachon, A. Verweij, D. Wollmann, A.-S. Mueller, and A. Bernhard, "Characterization of the radiation tolerance of cryogenic diodes for the High Luminosity LHC inner triplet circuit", Physical Review Accelerators and Beams 23, 053502, 2020, DOI: 10.1103/PhysRevAccelBeams.23.053502.

[22] E. Ravaioli, H. Bajas, V. I. Datskov, V. Desbiolles, J. Feuvrier, G. Kirby, M. Maciejewski, G. Sabbi, H. H. J. ten Kate, A. P. Verweij, "Protecting a Full-Scale Nb3Sn Magnet with CLIQ, the New Coupling-Loss-Induced Quench System", IEEE Trans. Appl. Supercond, DOI: 10.1109/TASC.2014.2364892.

[23] J. Steckert *et al*., "Application of the New Generic Quench Detection System for LHC's 11 T Dipole Magnet", IEEE Transactions on Applied Superconductivity, vol., DOI: 10.1109/TASC.2019.2898681.

[24] A. F. Lietzke *et al*., "Differentiation of performance-limiting voltage transients during Nb_3Sn magnet testing" AIP Conf. Proc., vol. 824, pp. 550–557, 2006, DOI: 10.1063/1.2192394.

[25] S. Bermudez et al., "Quench protection studies of the 11T Nb_3Sn dipole for LHC upgrades", IEEE Trans. Appl. Supercond. vol. 26, no. 4, Jun., 2016, DOI: 10.18429/JACoW-IPAC2014-WEPRI098.

[26] R. Garcia Alia, private communication, CERN Geneva, (2019).

[27] A. Antoine, D. Carrillo, R. Denz, F. Menendez Camara, F. Rodriguez Mateos, "Modifications to the protection system hardware to adapt to requirements given by the 11T dipoles installation in LHC", Internal Note 2019_08, EDMS: 2104676.

[28] M. Valette, "Parameters of Quench Heater (QH) circuits for all LHC Run II, Run III and HL-LHC superconducting magnets as well as their associated kicks on the beam", EDMS: 2051527.

[29] B. Lindstroem *et al*, "Fast failures in the LHC and future HL-LHC", DOI: 10.1103/PhysRevAccelBeams.23.081001.

[30] E. Ravaioli *et al*., "Lumped-element dynamic electro-thermal model of a superconducting magnet," Cryogenics, 2016, DOI: 10.1016/j.cryogenics.2016.04.004.